Two-step Optimal Allocation of Stationary and Mobile Energy Storage Systems in Resilient Distribution Networks

Xinyi Jiang, Jian Chen, Qiuwei Wu, Wen Zhang, Yicheng Zhang, and Jie Liu

***Abstract*—Energy storage systems (ESSs) are acknowledged to be a promising option to cope with issues in high penetration of renewable energy and guarantee a highly reliable power supply. In this paper, a two-step optimal allocation model is proposed to obtain the optimal allocation (location and size) of stationary ESSs (SESSs) and mobile ESSs (MESSs) in the resilient distribution networks (DNs). In the first step, a mixed-integer linear programming (MILP) problem is formulated to obtain the preselected location of ESSs with consideration of different scenarios under normal operation conditions. In the second step, a two-stage robust optimization model is established to get the optimal allocation results of ESSs under failure operation conditions which are solved by column-and-constraint generation (C&CG) algorithm. A hybrid ESS allocation strategy based on the subjective and objective weight analysis is proposed to give the final allocation scheme of SESSs and MESSs. Finally, the proposed two-step optimal allocation model is demonstrated on a modified IEEE 33-bus system to show its effectiveness and merits.**

***Index Terms*—Resilient distribution network, stationary energy storage system, mobile energy storage system, optimal allocation.**

NOMENCLATURE

A. Sets and Indices

κ	No. of scenario
Ω_L	Set of branches in distribution network (DN)
$\boldsymbol{\lambda}$, $\boldsymbol{\varpi}$	Dual variable sets
$\boldsymbol{d}$	Day set
$\boldsymbol{F}$	System operation set under disaster set of the second-step allocation
h	Number of iterations
$\boldsymbol{H}$	Planning decision set of the second-step allocation
i	Node
K	Scenario set
l	Branch
L_p	Set of branchs of p^{th} sub-district
N	Set of nodes in DN
p	Sub-district of DN
t	Time
T	Set of time
$\boldsymbol{U}$	Uncertainty set of the fault state of distribution lines in the second-step allocation
$\boldsymbol{x}$	First-stage decision variable vector of the second-step allocation
$\boldsymbol{y}_1$, $\boldsymbol{y}_2$	Second-stage decision variable vectors of the second-step allocation
z	Fault state scenario of distribution line

B. Parameters

α	Given discount rate of energy storage systems (ESSs)
α_{ess}	Growth rate of ESSs
π_{ess}	Capital recovery factor which converts the present investment costs into a stream of equal annual payments during planning period
η_{ch}, η_{dis}	Charging and discharging efficiencies
δ_i	Unit loss cost of load at node i
ϵ_i	The i^{th} class in elbow method
$\boldsymbol{A}$, $\boldsymbol{B}$, $\boldsymbol{C}$, $\boldsymbol{E}$, $\boldsymbol{D}_1$, $\boldsymbol{D}_2$, $\boldsymbol{F}_1$, $\boldsymbol{F}_2$	Coefficient matrices of the second-step allocation
$\boldsymbol{a}$, $\boldsymbol{b}_1$, $\boldsymbol{b}_2$	Coefficient column vectors
C_{sit}	Fixed cost for installing ESS

Manuscript received: December 28, 2020; accepted: May 26, 2021. Date of CrossCheck: May 26, 2021. Date of online publication: July 30, 2021.

This work was supported by the Science and Technology Project of State Grid Corporation of China "Research on resilience technology and application foundation of intelligent distribution network based on integrated energy system" (No. 52060019001H).

X. Jiang, J. Chen (corresponding author), and W. Zhang are with the Key Laboratory of Power System Intelligent Dispatch and Control of Ministry of Education, Shandong University, Jinan 250061, China (e-mail: Jiangxysdu@163.com; ejchen@sdu.edu.cn; zhangwen@sdu.edu.cn).

Q. Wu is with Center for Electric Power and Energy (CEE), Department of Electrical Engineering, Technical University of Denmark (DTU), 2800 Kongens Lyngby, Denmark (e-mail: qw@elektro.dtu.dk).

Y. Zhang is with the Institute for Infocomm Research (I2R), Agency for Science, Technology and Research (A*STAR), Singapore (e-mail: yzhang088@e.ntu.edu.sg).

J. Liu is with State Grid Yantai Power Supply Company, Yantai, China (e-mail: 568270937@qq.com).

DOI: 10.35833/MPCE.2020.000910

$C_{inv,1}$ Per-unit cost for energy capacity of installing ESS

$C_{inv,2}$ Per-unit cost for power capacity of installing ESS

$C_{o\&m}$ Unit capacity cost of operation and maintenance cost

C_{loss} Per-unit cost of DN loss

$\boldsymbol{d}$, $\boldsymbol{e}$, $\boldsymbol{g}$ Constant column matrices

$\underline{E}_{ess}$, $\bar{E}_{ess}$ The minimum and maximum ESS energy capacities

f_t^e Time-of-use price

k_s Sample in ϵ_i in elbow method

k_n Number of samples in ϵ_i in elbow method

K_p The maximum number of faults in the p^{th} subregion line

$l(i,:)$ Branch l which starts with node i

$l(:,i)$ Branch l which ends with node i

m_i Sample mean of ϵ_i in elbow method

M Big enough positive value

$\underline{N}_{ess}$, $\bar{N}_{ess}$ The minimum and maximum ESS numbers

N_y Total investment planning period

$\bar{P}_{ess}$ The maximum ESS power capacity

$P_i^{ch,\max}$ The maximum charging power at node i

$P_i^{dis,\max}$ The maximum discharging power at node i

$P_{i,t}^{pv,\max}$ Forecasted output active power of photovoltaic (PV) at node i at time t

$P_t^{sub,\max}$ The maximum output active power of substation at time t

$P_{i,\kappa,t}^{load}$, $Q_{i,\kappa,t}^{load}$ Active and reactive power demands of load at node i in scenario κ of the first step at time t

$P_{i,t}^{load}$, $Q_{i,t}^{load}$ Active and reactive power demands of load at node i of the second step at time t

$Q_{i,t}^{pv,\max}$ Forecasted output reactive power of PV at node i at time t

$Q_{i,t}^{pv,\min}$ The minimum reactive power of PV at node i at time t

$Q_t^{sub,\max}$ The maximum output reactive power of substation

R_l, X_l Resistance and reactance on branch l

$S_i^{PCS,\max}$ The maximum apparent power of energy storage converter of MESS at node i

$S_l^{\max}$ The maximum transmission capacity allowed on branch l

$SOC_{\max}$ The maximum state of charge (SOC) of ESS

$SOC_{\min}$ The minimum SOC of ESS

SOC_{ini} Initial SOC of ESS

$U_{\max}$ The maximum voltage magnitude

$U_{\min}$ The minimum voltage magnitude

$I_{\max}$ The maximum current magnitude of branch

U_0 Rated voltage value

C. Variables

η Auxiliary variable

$E_{i,\kappa,t}^{ess}$ Storage capacity of installed ESS at node i in scenario κ of the first step at time t

$E_{i,t}^{ess}$ Storage capacity of installed ESS at node i of the second step at time t

$E_{i,\kappa}^{inv,1}$ Energy capacity of installed ESS at node i in scenario κ of the first step

$E_i^{inv,2}$ Energy capacity of installed ESS at node i of the second step

$I_{2,l,\kappa,t}$ New defined variable of current on branch l in scenario κ at time t

$P_{i,\kappa}^{inv,1}$ Power capacity of installed ESS at node i of scenario κ in the first step

$P_i^{inv,2}$ Power capacity of installed ESS at node i of the second step

$P_{\kappa,t}^{sub}$, $Q_{\kappa,t}^{sub}$ Active and reactive power outputs of substation in scenario κ of the first step at time t

P_t^{sub}, Q_t^{sub} Active and reactive power outputs of substation of the second step at time t

$P_{l,\kappa,t}$, $Q_{l,\kappa,t}$ Active and reactive power on branch l in scenario κ of the first step at time t

$P_{l,t}$, $Q_{l,t}$ Active and reactive power on branch l of the second step at time t

$P_{i,\kappa,t}^{pv}$, $Q_{i,\kappa,t}^{pv}$ Active and reactive power of PV at node i in scenario κ of the first step at time t

$P_{i,t}^{pv}$, $Q_{i,t}^{pv}$ Active and reactive power of PV at node i of the second step at time t

$P_{i,\kappa,t}^{dis}$, $P_{i,\kappa,t}^{ch}$ Discharging and charging active power of ESS at node i in scenario κ of the first step at time t

$P_{i,t}^{dis}$, $P_{i,t}^{ch}$ Discharging and charging active power of ESS at node i of the second step at time t

$P_{i,\kappa,t}^{inj}$, $Q_{i,\kappa,t}^{inj}$ Active and reactive power injected by node i in scenario κ of the first step at time t

$P_{i,t}^{lr}$, $Q_{i,t}^{lr}$ The maximum recovery active and reactive loads of node i at time t

$Q_{i,\kappa,t}^{dis}$, $Q_{i,\kappa,t}^{ch}$ Discharging and charging reactive power of ESS at node i in scenario κ of the first step at time t

$Q_{i,t}^{dis}$, $Q_{i,t}^{ch}$ Discharging and charging reactive power of ESS at node i of the second step at time t

$U_{i,t}$ Voltage of node i at time t

$U_{2,i,\kappa,t}$ New defined variable of voltage at node i in scenario κ at time t

$x_{i,\kappa}^{inv,1}$ Flag bit of installed ESS at node i in scenario κ of the first step

$x_i^{inv,2}$ Flag bit of installed ESS at node i of the second step

$z_{l,t}$ Binary variable representing whether branch l is disconnected due to a fault at time t, which is equal to 1 when there is no fault on branch l at time t and 0 otherwise

D. Functions

f_κ	Objective function of the first-step allocation in scenario κ
f_κ^{inv}	Daily investment costs of the first-step allocation in scenario κ
f_κ^{pur}	Electricity purchase cost of the first-step allocation in scenario κ
f_κ^{loss}	Network loss cost of the first-step allocation in scenario κ
f^{inv}	Daily investment cost of the second-step allocation
f^{pur}	Electricity purchase cost of the second-step allocation
f^{load}	Daily comprehensive load loss cost of the second-step allocation

I. Introduction

ENERGY storage systems (ESSs) have been exploited for providing load shifting, voltage regulation, energy arbitrage, and other services to distribution networks (DNs). In addition to the common stationary energy storage systems (SESSs), mobile energy storage systems (MESSs) have also caught attention due to the mobility, flexibility, and supporting capability in power failure scenarios. The coexistence and development of SESSs and MESSs are expected to play an important role in future DNs, and the optimal allocation of SESSs and MESSs will be an attractive and complex problem which is vitally important to fully attest their advantages [1].

At present, most of the related literature mainly focuses on the optimal allocation of SESSs for different purposes, e.g., cost minimization [2]-[4], reliability enhancement [5], [6], voltage regulation [7], [8], peak load shaving [9], [10], etc. In [3], a hierarchical planning model with three interacting levels of battery ESSs is proposed to maximize the benefit of the distribution system operator. In [8], an ESS allocation method based on voltage sensitivity analysis is proposed to regulate voltage in a low-voltage DN. Reference [11] proposes a fitness-scaled chaotic artificial bee colony algorithm for the optimal placement of ESSs to enhance the reliability of the DN. Reference [12] proposes a hybrid ESS allocation model coordinating the hybrid ESS output power and the power reduction in the photovoltaic (PV) to smooth the active power variations of PVs. To solve the above problems, heuristic algorithms [13]-[16], mathematical programming [17], [18], and hybrid algorithms [19], [20] are generally adopted. Due to the seasonal variation of load and natural resources, typical scenarios are generally applied to obtain the optimal allocation scheme of ESSs for accommodating to different conditions. However, the final allocation is a kind of compromised scheme that may result in low utilization of some ESSs because of the requirement discrepancy of different scenarios. There might have potential limitations for allocating traditional SESSs and the emergence of MESSs provides a new choice.

Compared with SESSs, MESSs have flexible interfaces to support plug-and-play functionality, and the mobility of MESSs enables a single storage unit to achieve the tasks of multiple stationary units at different locations. The current research on MESSs focuses on optimal allocation and operation topics. In [21], a sizing and allocation algorithm for MESSs is proposed to maximize the distribution profit by considering the mobility of MESSs in multi-services of grid-support. In [22], a rolling integrated service restoration strategy is presented to minimize the total system cost by coordinating the scheduling of MESS fleets, resource dispatching of microgrids, and network reconfiguration of distribution systems. In [23], a two-stage optimization model is proposed to optimize the investments of MESS units and re-route the installed MESS units to form dynamic microgrids to enchance the resilience of DNs. In [24], a day-ahead energy management system for MESSs is proposed in which energy shifting and localized reactive power support are involved. Moreover, MESSs can serve as an emergency power supply during accidental failures and emergency repair works. However, the probability of DN failures is extremely low, and the emergency power supply allocated in the DNs will have the problems of resource redundancy and low utilization.

For the problem of low utilization in the allocation of SESSs, MESSs can be allocated to change access locations according to the variations of different operation scenarios. For the problem of resource redundancy in emergency power supply, MESSs can participate in the normal operation of DNs as well as serve as an emergency power supply when required. The hybrid allocation of MESSs and SESSs has the following advantages.

1) The number and capacity of the hybrid allocation of SESSs and MESSs will be decreased than that of single SESSs due to the mobility of MESSs.

2) The operation economy of DNs may be improved by changing access locations of MESSs to better meet the requirements of different scenarios.

3) The resilience of DNs can be enhanced through the transfers of MESSs to provide emergency power supply under failure operation conditions.

Based on the above analysis, a two-step optimal allocation model of SESSs and MESSs in the resilient DNs is proposed in this paper. First, *K*-means method is adopted to generate typical PV and load scenarios. Second, the ESSs are allocated under the normal and failure operation conditions of DNs, respectively. Finally, the optimal results of SESSs and MESSs are obtained by a hybrid ESS allocation strategy. The main contributions are summarized as follows.

1) A two-step optimal allocation model of SESSs and MESSs is proposed with consideration of the mobility and supporting capability of MESSs, which can improve the economy and resilience of DNs.

2) A mixed-integer linear programming (MILP) problem is formulated to obtain the preselected locations considering typical scenarios under normal operation conditions, and a two-stage robust optimization model is established to get the results considering the worst failure operation condition.

3) The combination weighting method based on the criteria importance through intercriteria correlation (CRITIC)

method and rank correlation analysis method is proposed, which considers the subjective weight of ESS installation locations as well as the objective weight with multiple impact factors.

The rest of the paper is organized as follows. Section II presents the optimization framework. Section III introduces the optimization model and problem formulation. The comparisons and analyses based on simulation results are presented in Section IV. Finally, the conclusions are drawn in Section V.

II. Optimization Framework

A two-step optimal allocation model of SESSs and MESSs in resilient DNs is proposed in this paper. The framework of the proposed model is shown in Fig. 1.

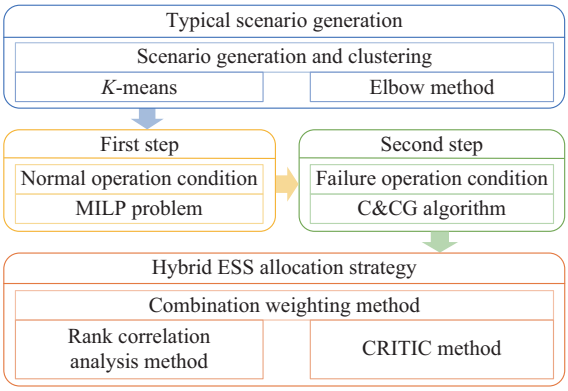

Fig. 1. Framework of proposed model.

First, some typical scenarios for the normal operation of DNs are generated based on the PV and load data of one year, which makes it possible to fully consider the variations of seasons, holidays, and weathers, etc.

Second, a two-step optimal allocation model is established. In the first step, an MILP problem under the normal operation condition is formulated to obtain the allocation results of all typical scenarios. In the second step, based on the candidate locations obtained in the first step, a two-stage robust optimization model is established to get the optimal allocation results under the failure operation condition of DNs, which is solved by the column-and-constraint generation (C&CG) algorithm.

Finally, the hybrid ESS allocation strategy is proposed to give the final scheme of SESSs and MESSs. The weight of each final installation location is given by a combination weighting method based on the CRITIC method and rank correlation analysis method, which considers the subjective and the objective weights with multiple impact factors. The final allocation results of SESSs and MESSs are obtained in accordance with the distance between locations in each district of DNs.

III. Optimization Model and Problem Formulation

A. Assumptions

In this paper, we make a set of necessary assumptions during the modeling process.

1) The PV and load data in this paper are inelastic, and the data deduced during the planning period according to the formula for scenario prediction are also inelastic.

2) In the moving route of MESSs, the electrical network is similar to the actual transportation network, and the adjacent contacts are the nearest moving routes.

3) In the second step of ESS allocation, a linearized DistFlow power flow model that ignores network losses is used. The network loss does not affect the final energy storage allocation result.

4) The lifetime of the network structure in the DN exceeds the expected life of the ESS, so as to ensure the effectiveness of the energy storage allocation during the planning period.

5) The electricity price will not be adjusted and fluctuated significantly during the planning period.

B. Generation of Typical Scenarios

In this paper, the *K*-means clustering method [25] is adopted to generate typical clustering scenarios, and the elbow method [26] is applied to determine the number of clusters. The elbow method uses the ratio of the average distance within a class (*nSE*) to the average distance between classes (*wSE*) as an index (*SE*) to describe the clustering error. Assuming the actual number of clusters is k, the elbow method model can be expressed as:

$$SE = \frac{nSE}{wSE} \tag{1}$$

$$nSE = \frac{1}{k}\sum_{i=1}^{k}\sum_{k_s \in \epsilon_i}\frac{\left|k_s - m_i\right|^2}{k_n} \tag{2}$$

$$wSE = \frac{2}{k(k-1)}\sum_{i=1}^{k}\sum_{j=i+1}^{k}\left|m_i - m_j\right|^2 \tag{3}$$

C. First-step ESS Allocation

The first-step ESS allocation refers to the optimal ESS allocation under the normal operation condition of DNs. The main function of ESSs in DNs is to enhance the utilization of PV and increase the operation economy through time-varying electricity prices. This paper establishes the optimal allocation model of the first step based on typical scenarios. The first-step allocation problem in scenario κ is formulated as:

$$\min_{\kappa \in K} f_\kappa = f_\kappa^{inv} + f_\kappa^{pur} + f_\kappa^{loss} \tag{4}$$

$$f_\kappa^{inv} = \sum_{i \in N}\pi_{ess}\left(C_{sit}x_{i,\kappa}^{inv,1} + C_{inv,1}E_{i,\kappa}^{inv,1} + C_{inv,2}P_{i,\kappa}^{inv,1}\right) + C_{o\&m}P_{i,\kappa}^{inv,1} \tag{5}$$

$$f_\kappa^{pur} = \sum_{t=1}^{T}P_{\kappa,t}^{sub}f_t^e \tag{6}$$

$$f_\kappa^{loss} = C_{loss}\sum_{t=1}^{T}\sum_{l(i,j)\in\Omega_L}I_{2,l,\kappa,t}R_l \tag{7}$$

$$\pi_{ess} = \frac{r(1+r)^{N_y}}{(1+r)^{N_y}-1} \tag{8}$$

$$r = \frac{1+\alpha}{(1+\alpha_{ess})-1} \tag{9}$$

s.t.

$$\underline{N}_{ess} \le \sum_{i \in N} x_{i,\kappa}^{inv,1} \le \bar{N}_{ess} \tag{10}$$

$$x_{i,\kappa}^{inv,1}\,\underline{E}_{ess} \le E_{i,\kappa}^{inv,1} \le x_{i,\kappa}^{inv,1}\,\bar{E}_{ess} \tag{11}$$

$$0 \le P_{i,\kappa}^{inv,1} \le x_{i,\kappa}^{inv,1}\,\bar{P}_{ess} \tag{12}$$

$$\begin{cases} \sum\limits_{l(i,:)\in\Omega_L} P_{l,\kappa,t} - \sum\limits_{l(:,i)\in\Omega_L} (P_{l,\kappa,t} - I_{2,l,\kappa,t}R_l) = P_{i,\kappa,t}^{inj} \\ \sum\limits_{l(i,:)\in\Omega_L} Q_{l,\kappa,t} - \sum\limits_{l(:,i)\in\Omega_L} (Q_{l,\kappa,t} - I_{2,l,\kappa,t}X_l) = Q_{i,\kappa,t}^{inj} \end{cases} \tag{13}$$

$$U_{2,j,\kappa,t} = U_{2,i,\kappa,t} - 2(P_{l,\kappa,t}R_l + Q_{l,\kappa,t}X_l) + I_{2,l,\kappa,t}(R_l^2 + X_l^2) \tag{14}$$

$$\left\| \begin{bmatrix} 2P_{l,\kappa,t} \\ 2Q_{l,\kappa,t} \\ I_{2,l,\kappa,t} - U_{2,i,\kappa,t} \end{bmatrix} \right\|_2 \le I_{2,l,\kappa,t} + U_{2,i,\kappa,t} \tag{15}$$

$$\begin{cases} P_{i,\kappa,t}^{inj} = P_{\kappa,t}^{sub} + P_{i,\kappa,t}^{pv} + P_{i,\kappa,t}^{dis} - P_{i,\kappa,t}^{ch} - P_{i,\kappa,t}^{load} \\ Q_{i,\kappa,t}^{inj} = Q_{\kappa,t}^{sub} + Q_{i,\kappa,t}^{pv} + Q_{i,\kappa,t}^{dis} - Q_{i,\kappa,t}^{ch} - Q_{i,\kappa,t}^{load} \end{cases} \tag{16}$$

$$U_{\min}^2 \le U_{2,i,\kappa,t} \le U_{\max}^2 \tag{17}$$

$$0 \le I_{2,l,\kappa,t} \le I_{\max}^2 \tag{18}$$

$$0 \le P_{i,\kappa,t}^{ch} \le P_{i,\kappa}^{inv,1} \tag{19}$$

$$0 \le P_{i,\kappa,t}^{dis} \le P_{i,\kappa}^{inv,1} \tag{20}$$

$$(P_{i,\kappa,t}^{ch})^2 + (Q_{i,\kappa,t}^{ch2})^2 \le (S_i^{PCS,\max})^2 \tag{21}$$

$$(P_{i,\kappa,t}^{dis})^2 + (Q_{i,\kappa,t}^{dis})^2 \le (S_i^{PCS,\max})^2 \tag{22}$$

$$E_{i,\kappa,t+1}^{ess} = E_{i,\kappa,t}^{ess} + \eta_{ch}P_{i,\kappa,t}^{ch} - P_{i,\kappa,t}^{dis}/\eta_{dis} \tag{23}$$

$$SOC_{\min} \cdot E_{i,\kappa}^{inv,1} \le E_{i,\kappa,t}^{ess} \le SOC_{\max} \cdot E_{i,\kappa}^{inv,1} \tag{24}$$

$$E_{i,\kappa,1}^{ess} = SOC_{ini} \cdot E_{i,\kappa}^{inv,1} \tag{25}$$

$$0 \le P_{i,\kappa,t}^{sub} \le P_t^{sub,\max} \tag{26}$$

$$0 \le Q_{i,\kappa,t}^{sub} \le Q_t^{sub,\max} \tag{27}$$

$$0 \le P_{i,\kappa,t}^{pv} \le P_{i,t}^{pv,\max} \tag{28}$$

$$Q_{i,t}^{pv,\min} \le Q_{i,\kappa,t}^{pv} \le Q_{i,t}^{pv,\max} \tag{29}$$

The investment costs f_κ^{inv} in (5) include the fixed ESS costs, variable ESS costs of energy capacity and power capacity, and operation and maintenance costs in scenario κ. The constraints can be divided into investment constraints (10)-(12) and operation constraints (13)-(29). Specifically, constraints (10)-(12) bound the total number, energy capacity, and power capacity of the ESS, respectively. The optimal power flow model based on the second-order cone programming (SOCP) is adopted, which is shown in constraints (13)-(16). Constraints (17) and (18) impose limits on the voltage and current to ensure the secure operation of DNs. Constraints (19)-(24) are the power and energy-relevant limits of the ESS. It should be noted that binary variables are not needed to avoid simultaneous charging and discharging of ESSs when the roundtrip efficiency is smaller than 1 [27]. Constraint (25) sets the initial state of charge (SOC). Constraints (26) and (27) impose the limits on the active and reactive power of DNs when purchasing electricity from the power grid. Constraints (28) and (29) impose the active and reactive power limits on PVs of DNs.

D. Second-step ESS Allocation

The second-step ESS allocation refers to the optimal ESS allocation under the failure operation condition of DNs. Based on the uncertainty set of the multi-area line failures, this paper establishes a two-stage robust optimization model under the failure operation condition of DNs to pursue the optimal ESS allocation scheme which guarantees the uninterrupted power supply of critical loads under the worst failure condition. Therefore, the objective function of ESS allocation in the second step is to minimize the investment cost and the annual comprehensive load loss cost under the worst failure condition.

In the two-stage robust optimization model, the first-stage optimization is based on the outer-layer function min(·) to formulate the ESS allocation scheme on the preselected locations of the first-step allocation results. In the second-stage optimization, the middle-layer function max(·) is used to find the worst condition which maximizes the load loss cost in the uncertain set of line failures. Then, the inner-layer function min(·) minimizes the load loss cost of DNs under the worst failure condition. In summary, the optimal ESS allocation model can be modeled by the three-layer "min-max-min" function. The outer layer is the planning decision set, and the variables are ESS allocation variables. The middle layer is the uncertainty set of line failures, and the variables are failure state variables. The inner layer is the system operation set, and the variables are system operation variables. The problem is formulated as:

$$\min\left(f^{inv} + \max\left(\min\left(f^{load} + f^{pur}\right)\right)\right) \tag{30}$$

$$f^{inv} = \sum_{i \in N} \pi_{ess}\left(C_{sit}x_i^{inv,2} + C_{inv,1}E_i^{inv,2} + C_{inv,2}P_i^{inv,2}\right) + C_{o\&m}P_i^{inv,2} \tag{31}$$

$$f^{load} = \sum_{t=1}^{T}\sum_{i=1}^{N} \delta_i\left(P_{i,t}^{load} - P_{i,t}^{lr}\right) \tag{32}$$

$$f^{pur} = \sum_{t=1}^{T} P_t^{sub} f_t^e \tag{33}$$

s.t.

$$\underline{N}_{ess} \le \sum_{i \in N} x_i^{inv,2} \le \bar{N}_{ess} \tag{34}$$

$$x_i^{inv,2}\,\underline{E}_{ess} \le E_i^{inv,2} \le x_i^{inv,2}\,\bar{E}_{ess} \tag{35}$$

$$0 \le P_i^{inv,2} \le x_i^{inv,2}\,\bar{P}_{ess} \tag{36}$$

$$0 \le P_{i,t}^{dis} \le P_i^{inv,2} \tag{37}$$

$$SOC_{\min} \cdot E_i^{inv,2} \le E_{i,t}^{ess} \le SOC_{\max} \cdot E_i^{inv,2} \tag{38}$$

$$E_{i,t+1}^{ess} = E_{i,t}^{ess} - \frac{P_{i,t}^{dis}\Delta t}{\eta_{dis}} \tag{39}$$

$$E_{i,1}^{ess} = SOC_{ini} \cdot E_i^{inv,2} \tag{40}$$

$$\sum_{l \in l(:,i)} P_{l,t} - \sum_{l \in l(i,:)} P_{l,t} = -P_t^{sub} - P_{i,t}^{pv} - P_{i,t}^{dis} + P_{i,t}^{lr} \tag{41}$$

$$\sum_{l \in l(:,i)} Q_{l,t} - \sum_{l \in l(i,:)} Q_{l,t} = -Q_t^{sub} - Q_{i,t}^{pv} - Q_{i,t}^{dis} + Q_{i,t}^{lr} \tag{42}$$

$$U_{i,t} - U_{j,t} \le M(1 - z_{l,t}) + \frac{R_l P_{l,t} + X_l Q_{l,t}}{U_0} \tag{43}$$

$$U_{i,t}-U_{j,t}\geq -M(1-z_{l,t})+\frac{R_l P_{l,t}+X_l Q_{l,t}}{U_0} \tag{44}$$

$$-z_{l,t}S_l^{\max}\leq P_{l,t}\leq z_{l,t}S_l^{\max} \tag{45}$$

$$-z_{l,t}S_l^{\max}\leq Q_{l,t}\leq z_{l,t}S_l^{\max} \tag{46}$$

$$-\sqrt{2}\,z_{l,t}S_l^{\max}\leq P_{l,t}+Q_{l,t}\leq \sqrt{2}\,z_{l,t}S_l^{\max} \tag{47}$$

$$-\sqrt{2}\,z_{l,t}S_l^{\max}\leq P_{l,t}-Q_{l,t}\leq \sqrt{2}\,z_{l,t}S_l^{\max} \tag{48}$$

$$U_{\min}\leq U_{i,t}\leq U_{\max} \tag{49}$$

$$0\leq P_{i,t}^{lr}\leq P_{i,t}^{load} \tag{50}$$

$$0\leq Q_{i,t}^{lr}\leq Q_{i,t}^{load} \tag{51}$$

$$U=z_{l,t}\left|\sum_{l\in L_p}(1-z_{l,t})\leq K_p\right. \tag{52}$$

The constraints (37)-(40) represent the ESS operation model as the emergency power. The linearized DistFlow model is adopted in the second-step allocation and the Big-*M* method is used to relax the voltage constraint due to line failures. The power flow model of DNs can be expressed as constraints (41)-(48). Constraints (50) and (51) impose limits on an active or reactive load of DN restoration. A large DN can be roughly divided into several sub-regions. Line failures in different districts in DNs are limited by the maximum number of line failures. The model of the line uncertainty set of each sub-region in DNs can be expressed as (52).

The two-stage robust optimization model can be re-formulated into the following matrix form.

$$\min_{\boldsymbol{x}\in\boldsymbol{H}}\boldsymbol{a}^{\mathrm{T}}\boldsymbol{x}+\max_{\boldsymbol{z}\in\boldsymbol{U}}\min_{\boldsymbol{y}_1,\boldsymbol{y}_2\in\boldsymbol{F}(\boldsymbol{x},\boldsymbol{z})}(\boldsymbol{b}_1^{\mathrm{T}}\boldsymbol{y}_1+\boldsymbol{b}_2^{\mathrm{T}}\boldsymbol{y}_2) \tag{53}$$

s.t.

$$\boldsymbol{A}\boldsymbol{x}\leq\boldsymbol{d} \tag{54}$$

$$\boldsymbol{B}\boldsymbol{x}+\boldsymbol{C}\boldsymbol{u}+\boldsymbol{D}_1\boldsymbol{y}_1+\boldsymbol{D}_2\boldsymbol{y}_2\geq\boldsymbol{e} \tag{55}$$

$$\boldsymbol{E}\boldsymbol{x}+\boldsymbol{F}_1\boldsymbol{y}_1+\boldsymbol{F}_2\boldsymbol{y}_2=\boldsymbol{g} \tag{56}$$

where $\boldsymbol{y}_1$ is the vector of non-negative variables such as $P_{i,t}^{lr}$, $Q_{i,t}^{lr}$; and $\boldsymbol{y}_2$ is the vector of real variables such as $P_{l,t}$, $Q_{l,t}$. Formula (53) represents the objective function (30); (54) represents constraints (34)-(36) of the planning decision set $\boldsymbol{H}$; (55) represents (26)-(29), (37)-(38), (43)-(52) of the system operation set under disaster $\boldsymbol{F}$; and (56) represents (39)-(42) of the system operation set under disaster $\boldsymbol{F}$. The C&CG algorithm [28] is adopted to solve the two-stage robust optimization model proposed in this paper.

First, the two-stage robust optimization model is decomposed into a main problem and a sub-problem. The main problem is to plan the ESS allocation scheme under a given line failure condition $\boldsymbol{u}^*$ in the DN, which is presented as:

$$\begin{cases}\max(\boldsymbol{a}^{\mathrm{T}}\boldsymbol{x}+\eta)\\ \text{s.t. }\boldsymbol{A}\boldsymbol{x}\leq\boldsymbol{d}\\ \quad\eta\geq\boldsymbol{b}_1^{\mathrm{T}}\boldsymbol{y}_1+\boldsymbol{b}_2^{\mathrm{T}}\boldsymbol{y}_2\\ \quad\boldsymbol{B}\boldsymbol{x}+\boldsymbol{C}\boldsymbol{u}^*+\boldsymbol{D}_1\boldsymbol{y}_1^h+\boldsymbol{D}_2\boldsymbol{y}_2^h\geq\boldsymbol{e}\\ \quad\boldsymbol{E}\boldsymbol{x}+\boldsymbol{F}_1\boldsymbol{y}_1^h+\boldsymbol{D}_2\boldsymbol{y}_2^h=\boldsymbol{g}\end{cases} \tag{57}$$

The sub-problem is to find the worst failure condition of distribution line when the decision variables in the planning scheme $\boldsymbol{x}^*$ of the main problem are known. The specific form is as follows:

$$\begin{cases}\max(\min(\boldsymbol{b}_1^{\mathrm{T}}\boldsymbol{y}_1+\boldsymbol{b}_2^{\mathrm{T}}\boldsymbol{y}_2))\\ \text{s.t. }\boldsymbol{B}\boldsymbol{x}^*+\boldsymbol{C}\boldsymbol{u}+\boldsymbol{D}_1\boldsymbol{y}_1^h+\boldsymbol{D}_2\boldsymbol{y}_2^h\geq\boldsymbol{e}\quad(\boldsymbol{\lambda})\\ \quad\boldsymbol{E}\boldsymbol{x}^*+\boldsymbol{F}_1\boldsymbol{y}_1^h+\boldsymbol{D}_2\boldsymbol{y}_2^h=\boldsymbol{g}\quad(\boldsymbol{\varpi})\\ \quad\boldsymbol{u}\in\boldsymbol{U}\end{cases} \tag{58}$$

Note that the above sub-problem is a two-layer optimization problem, and the inner min(·) problem is a convex optimization problem with strong duality. According to the principle of duality, the inner min(·) problem is dualized to max(·), and a bipolar problem is transformed into a unipolar problem. The specific form of the dual problem is as follows:

$$\begin{cases}\max((\boldsymbol{e}-\boldsymbol{B}\boldsymbol{x}^*-\boldsymbol{C}\boldsymbol{u})^{\mathrm{T}}\boldsymbol{\lambda}+(\boldsymbol{g}-\boldsymbol{E}\boldsymbol{x}^*)^{\mathrm{T}}\boldsymbol{\varpi})\\ \text{s.t. }\boldsymbol{D}_1^{\mathrm{T}}\boldsymbol{\lambda}+\boldsymbol{F}_1^{\mathrm{T}}\boldsymbol{\varpi}\leq\boldsymbol{b}_1\\ \quad\boldsymbol{D}_2^{\mathrm{T}}\boldsymbol{\lambda}+\boldsymbol{F}_2^{\mathrm{T}}\boldsymbol{\varpi}\leq\boldsymbol{b}_2\\ \quad\boldsymbol{\lambda}\geq\boldsymbol{0}\\ \quad\boldsymbol{u}\in\boldsymbol{U}\end{cases} \tag{59}$$

The objective function in (59) contains non-linear variables in the form of a product of variables. This paper uses the Big-*M* method to linearize this function. For the product of the binary variable U_k and the continuous variable Z_k, the linearized constraint can be obtained by introducing an auxiliary variable V_k and then relaxed by the Big-*M* method [29]. The flowchart of the C&CG algorithm is shown in Fig. 2.

$$-MU_k\leq V_k\leq MU_k \tag{60}$$

$$Z_k-M(1-U_k)\leq V_k\leq Z_k+M(1-U_k) \tag{61}$$

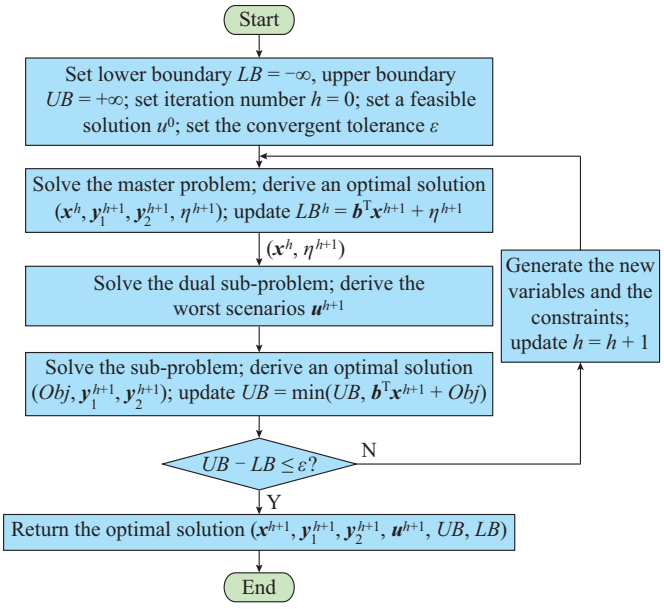

Fig. 2. Flowchart of C&CG algorithm.

As shown in Table I, the operation and allocation variables of the first- and second-step ESS allocations in this paper are different. After the optimal allocation of the first step, the results of the ESS allocation in six scenarios and the spatial location of each candidate node are obtained. In

the second step of the ESS allocation, the ESS allocation results in the case of failure are obtained from the ESS candidate nodes obtained in the first step.

TABLE I
OPERATION AND ALLOCATION VARIABLES OF EACH SUB-PROBLEM

Allocation	Operation variable	Allocation variable
First-step ESS allocation	$P_{\kappa,t}^{sub}$, $Q_{\kappa,t}^{sub}$, $U_{2,i,\kappa,t}$, $I_{2,l,\kappa,t}$, $P_{l,\kappa,t}$, $Q_{l,\kappa,t}$, $P_{i,\kappa,t}^{pv}$, $Q_{i,\kappa,t}^{pv}$, $P_{i,\kappa,t}^{dis}$, $Q_{i,\kappa,t}^{dis}$, $P_{i,\kappa,t}^{ch}$, $Q_{i,\kappa,t}^{ch}$	$x_{i,\kappa}^{inv,1}$, $E_{i,\kappa}^{inv,1}$, $P_{i,\kappa}^{inv,1}$
Second-step ESS allocation	$P_{i,t}^{lr}$, $Q_{i,t}^{lr}$, P_t^{sub}, Q_t^{sub}, $P_{i,t}^{pv}$, $Q_{i,t}^{pv}$, $P_{i,t}^{dis}$, $Q_{i,t}^{dis}$, $P_{l,t}$, $Q_{l,t}$, $U_{i,t}$, $z_{l,t}$	$x_i^{inv,2}$, $E_i^{inv,2}$, $P_i^{inv,2}$

E. A Hybrid ESS Allocation Strategy

After the two-step ESS allocation, the results are screened using the proposed hybrid ESS allocation strategy to obtain the optimal hybrid ESS allocation scheme. First, the subjective and objective combination weighting method is applied to analyze the m preselected ESS allocation nodes to obtain the weight order of m locations. The objective weight analysis is carried out and the CRITIC method [30] is used. The rank correlation analysis method [31] is combined with the geographic location of each node to perform subjective weight analysis. Second, according to the weight results of m locations, the first E ESS allocation nodes are selected. The SESSs and MESSs are determined according to the distance from the $m-E$ remaining candidate nodes in each district to the E determined allocation nodes. The flowchart of proposed hybrid ESS allocation strategy is shown in Fig. 3, which follows several important principles.

1) In each district, it is necessary to allocate at least one MESS in order to ensure that the ESS can be used as an emergency power source.

2) The total number of ESSs installed in the district needs to be proportional to the total number of nodes in this district.

3) The ESS installation locations that are close to the candidate locations are given priority to install MESSs in order to ensure that the optimal hybrid allocation results can meet the requirements of different scenarios in DNs.

4) The nodes of the critical load are given priority to allocate SESSs.

5) Candidate locations that are not equipped with ESSs need to be equipped with MESS installation interfaces.

6) The installed capacity of MESS and SESS is allocated with the maximum installed capacity in various operation scenarios.

IV. CASE STUDY

The proposed model is tested based on a modified IEEE 33-node DN, as shown in Fig. 4. The proposed MILP problem is solved in Gurobi 8.1.1. We use MATLAB R2018a to formulate the desired model which is then linked with Gurobi solver. The simulation is carried out on a PC with Intel Quad Core 2.70 GHz and 8 GB RAM.

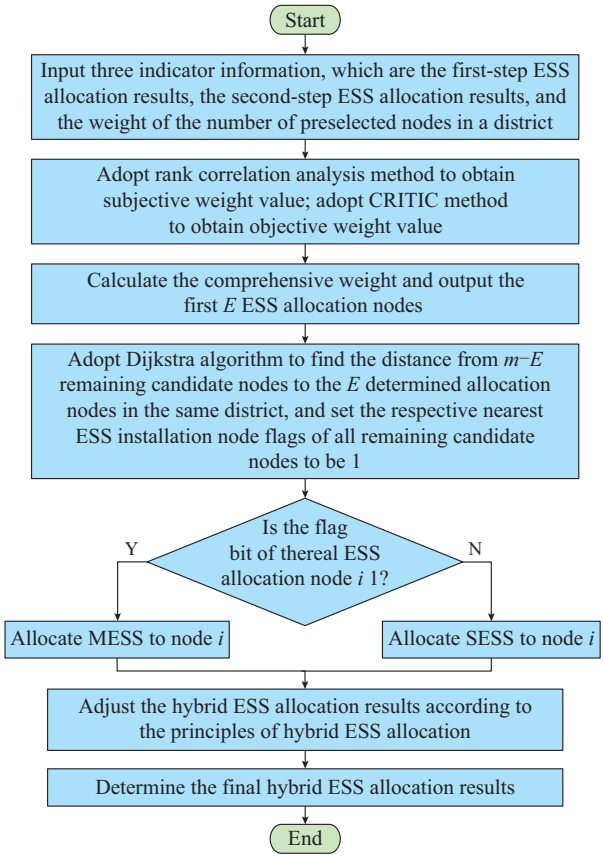

Fig. 3. Flowchart of proposed hybrid ESS allocation strategy.

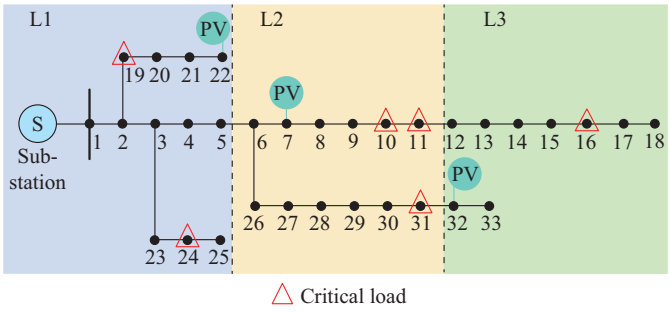

Fig. 4. Modified IEEE 33-node DN.

A. Test System Information

The reference voltage of the test system is 12.66 kV, the allowable range of node voltage is 0.9-1.1 p.u., and other system parameters can be found in [32]. The capacities of the three PV generators located at buses 7, 22, and 32 are 500 kW, 600 kW, and 500 kW, respectively. The DN area is divided into three districts according to the locations shown in Fig. 4, i.e., L1, L2, and L3.

The time-of-use (TOU) price of DNs is shown in Fig. 5(a), and the typical daily load of DNs is shown in Fig. 5(b) [7]. The planning period is 10 years and the investments are determined at the beginning of the planning horizon. The per-unit capacity investment costs for ESSs are set to be $C_{inv,1}=300$ \$/kWh and $C_{inv,2}=250$ \$/kW. The fixed cost for installing an ESS is 10% of its energy capacity costs, i.e., $C_{inv,1}=0.1C_{inv,2}E_i^{inv}$. The fixed cost of MESSs is about 2%

higher than that of SESSs due to the flexible interfaces. The annual operation and maintenance cost $C_{o\&m}$ is 5% of the power capacity investment cost $C_{inv,2}$, i.e., $C_{o\&m}=0.05C_{inv,2}$. As for other financial parameters, the discount rate α is assumed to be 5% and the growth rate of the investment cost α_{ess} is assumed to be −1%, i.e., the cost will decrease over the years. In the first step of normal operation, the given maximum ESS configuration node is 6. The SOC change range of the ESS is 0.10-0.95 and the initial SOC is 0.2. The charging/discharging efficiency is 0.95. The maximum allocation capacity of the ESS is 5 MWh and the maximum allocation power is 1.5 MW. The initial SOC of the second-step ESS allocation is 0.9, and the failure duration is 2 hours. The average moving cost of the MESS between scenario transitions is \$600 per time. $K_p=2$.

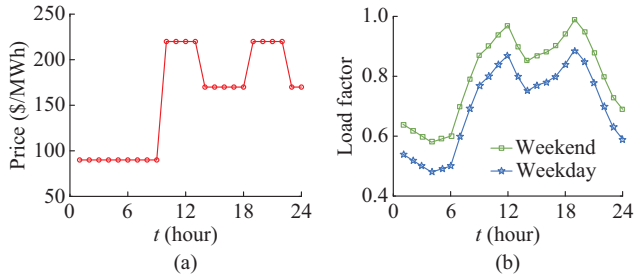

Fig. 5. Information of DNs. (a) TOU price. (b) Typical daily load.

B. Result Analysis

Based on the *K*-means clustering method, the PV and load data of scenario clustering are demonstrated in Fig. 6, where the blue line represents the change curve of PV and load in one year (365 days), and the white line represents the change curve of PV and load in the six typical scenarios obtained by clustering. The clustering errors changing with the number of clusters are shown in Fig. 7. Considering the real scenarios, the data clustering of the DN for a year is generally divided into 4 categories according to the season. The selected number of clusters should be able to describe more than 4 scenarios. In addition, the larger the number of clusters, the smaller the clustering error. Combined with the clustering error curve shown in Fig. 7, the optimal number of clusters for PV and load data in one year is determined by the elbow method, which turns out to be 6.

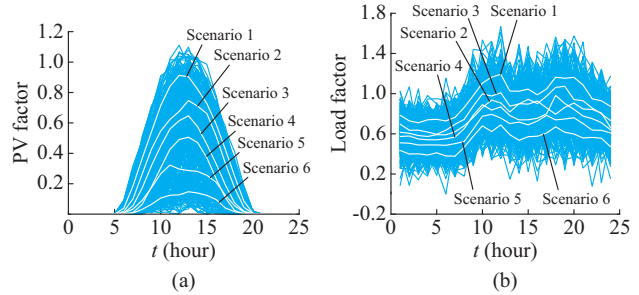

Fig. 6. PV and load data of scenario clustering. (a) PV data. (b) Load data.

According to the obtained six typical PV and load scenarios, the ESS allocation under the normal operation condition in the first step is performed.

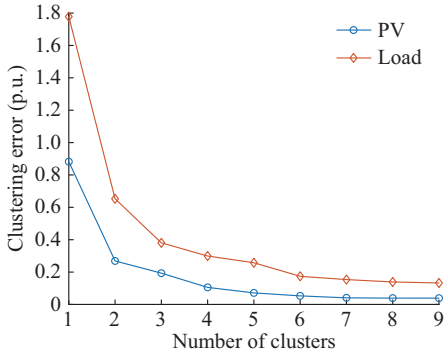

Fig. 7. Clustering error curves.

The first-step ESS allocation results for the six scenarios are shown in Table II. The main role of the ESSs in the first step is to accommodate more PVs and realize arbitrage by the TOU price. The SOC curves of the ESS in scenario 1 are shown in Fig. 8.

TABLE II
FIRST-STEP ESS ALLOCATION RESULTS FOR SIX SCENARIOS

Scenario	Allocation node	Power (kW)	Capacity (kWh)
1	2, 8, 14, 25, 30, 32	500, 300, 500, 500, 600, 200	1600, 1100, 1600, 1500, 1900, 600
2	2, 10, 14, 24, 25, 30	1400, 100, 100, 200, 130, 400	4600, 300, 300, 600, 400, 1400
3	2, 8, 14, 24, 25, 30	500, 300, 500, 300, 350, 800	1600, 900, 1800, 900, 1700, 2600
4	2, 12, 14, 24, 25, 30	1000, 100, 100, 140, 100, 400	3300, 300, 300, 500, 370, 1200
5	8, 14, 24, 25, 30, 32	200, 300, 200, 200, 700, 200	600, 1100, 800, 700, 2300, 600
6	2, 14, 24, 25, 30, 32	700, 500, 200, 200, 600, 200	2300, 1800, 700, 700, 2000, 600

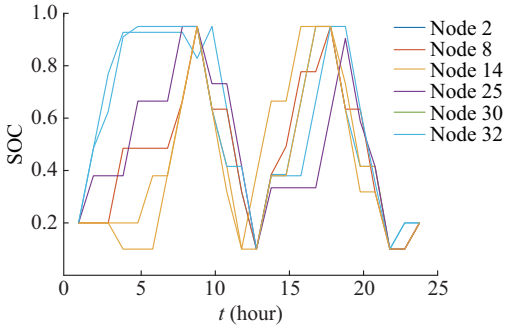

Fig. 8. SOC curves of ESS in scenario 1.

The pre-selected allocation locations of ESSs obtained in the first step have nine locations in total, which are nodes 2, 8, 10, 12, 14, 24, 25, 30, and 32. The total locations obtained in the first step are regarded as the pre-selection of the ESS allocation locations for the second step. This paper sets four failure scenarios and the second-step ESS allocation results are shown in Table III. The all load recovery rate (ALRR) and critical load recovery rate (CLRR) of the four failure scenarios are shown in Table IV. Taking failure scenario 4 as an example, the convergence process of the

C&CG algorithm is shown in Fig. 9.

TABLE III
SECOND-STEP ESS ALLOCATION RESULTS

Failure scenario	Allocation node	Power (kW)	Capacity (kWh)
1	2, 8, 24, 32	50, 100, 240, 100	150, 300, 700, 300
2	2, 12, 24, 32	30, 50, 400, 80	80, 130, 1030, 220
3	2, 10, 24, 30	300, 100, 400, 30	600, 300, 1000, 100
4	2, 8, 24, 32	100, 100, 400, 250	300, 300, 1000, 400

TABLE IV
DN RESTORATION RESULTS IN DIFFERENT FAILURE SCENARIOS

Failure scenario	Fault line	ALRR (%)	CLRR (%)
1	1, 2, 5, 9, 14, 15	20.73	80.00
2	1, 2, 5, 8, 12, 15	21.84	86.79
3	1, 2, 5, 13, 14, 30	21.84	82.46
4	1, 3, 5, 8, 12, 15	20.59	80.00

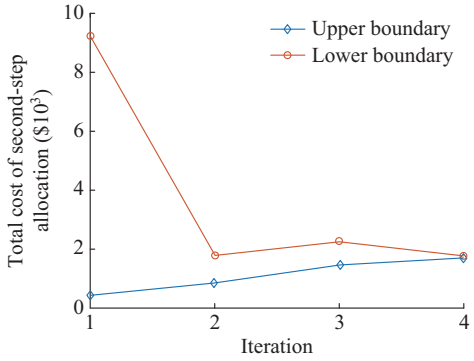

Fig. 9. Convergence process of C&CG algorithm.

The worst failure operation condition is the failures of fault 1, 3, 5, 8, 12, and 15. The CLRR is 80% and the ALRR is 20.59%. Under the worst failure operation condition of DNs, the ESS can facilitate operation the load recovery which can ensure the reliability of the power supply for important loads and improve the safety of the DN operation.

Taking the first-step ESS allocation results, the second-step ESS allocation results, and the location of each node as the index of each ESS allocation location, the combination weighting method based on the CRITIC method and rank correlation analysis method is adopted to obtain the comprehensive weight, which is shown in Table V.

TABLE V
COMPREHENSIVE WEIGHT OF ESS ALLOCATION NODES

Node	Weight	Node	Weight
2	0.2839	24	0.0760
8	0.1812	25	0.0620
10	0.1444	30	0.0288
12	0.0995	32	0.0288
14	0.0953		

According to the comprehensive weight of each candidate location, the locations expected to install ESSs are selected as nodes 2, 30, 24, 32, 14, and 25. With consideration of the principles in the hybrid ESS allocation strategy, the final hybrid ESS allocation results are shown in Fig. 10 and Table VI. In L1 district, node 24 is installed with MESS and node 2 is installed with SESS. The candidate node 25 can utilize the installed MESS of node 24 which is able to move according to requirements. In L2 district, node 8 is installed with MESS and node 30 is installed with SESS. In different operation scenarios, the MESS installed in node 8 can be moved to node 10. In L3 district, node 14 is installed with MESS and node 32 is installed with SESS. The candidate node 12 can share the MESS installed in node 14 in different scenarios.

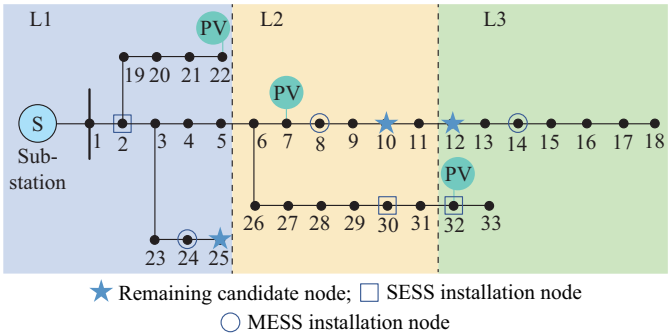

Fig. 10. Hybrid ESS allocation results.

TABLE VI
HYBRID ESS ALLOCATION RESULTS

Type	Allocation node	Power (kW)	Capacity (kWh)
SESS	2, 30, 32	1400, 700, 200	4600, 2300, 600
MESS	8, 14, 24	300, 500, 300	1100, 1800, 900

In order to verify the correctness and effectiveness of the proposed hybrid ESS allocation strategy, three allocation strategies are demonstrated for comparison and verification. Strategy 1 is to allocate SESS for a single scenario under normal and failure operation conditions; strategy 2 is to allocate SESS for multiple scenarios under normal and failure operation conditions; and strategy 3 is to allocate SESS only considering the normal operation condition of DNs. The allocation results of the strategies 1-3 are shown in Table VII. Figure 11 shows the annual operation costs of the different allocation strategies under normal operation conditions of DNs. Taking failure scenario 4 in Table IV as an example, the SOC of ESSs in the DN are shown in Fig. 12.

TABLE VII
ALLOCATION RESULTS OF ALLOCATION STRATEGIES 1-3

Strategy	Allocation node	Power (kW)	Capacity (kWh)
1	2, 11, 14, 24, 25, 30	900, 160, 400, 200, 180, 700	2800, 520, 1400, 650, 600, 2400
2	2, 8, 14, 24, 30, 32	1400, 300, 500, 300, 700, 200	4600, 1100, 1800, 900, 2300, 600
3	2, 8, 14, 24, 25, 30	1400, 300, 500, 300, 500, 700	4600, 1100, 1800, 900, 1500, 2300

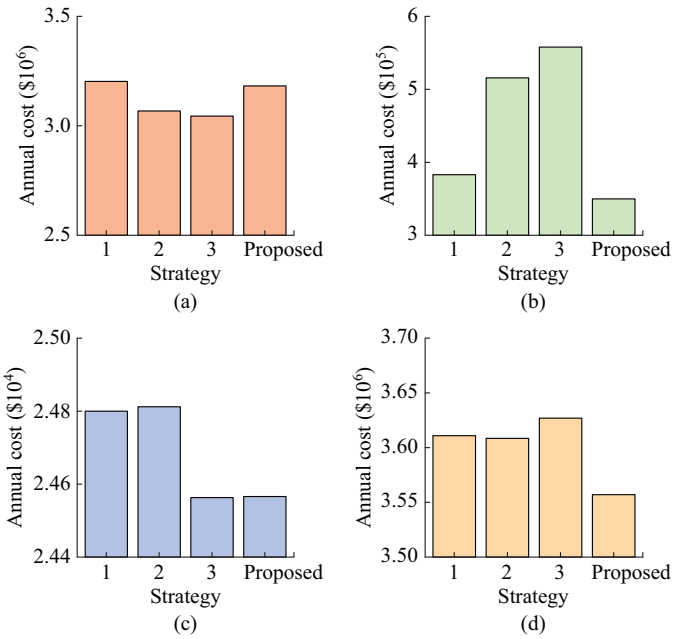

Fig. 11. Annual operation cost. (a) Electricity purchase cost. (b) ESS allocation cost. (c) Network loss cost. (d) Total annual operation cost.

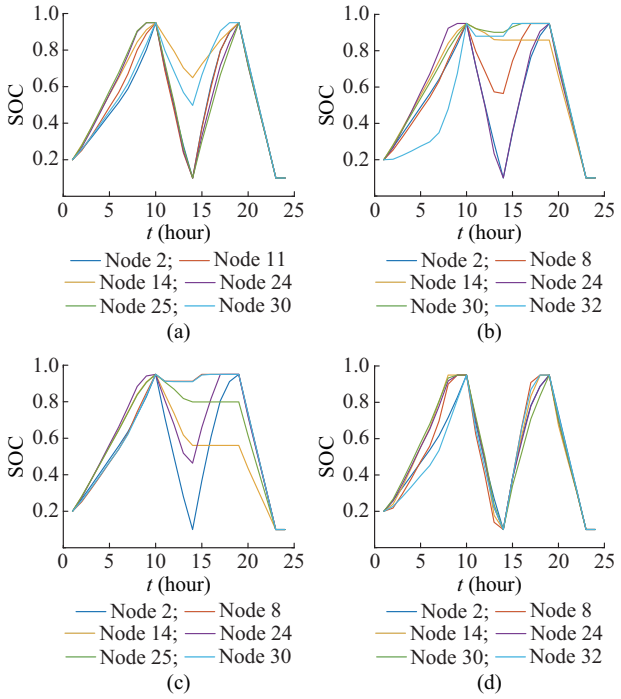

Fig. 12. SOC of ESSs in failure scenario 4. (a) Strategy 1. (b) Strategy 2. (c) Strategy 3. (d) Proposed strategy.

In Fig. 11(a), the power purchase cost of strategy 1 is the highest, and the single-scenario ESS allocation result cannot guarantee the optimal operation in multiple scenarios, which verifies the effectiveness of the multi-scenario method. In Fig. 11(b), although the power purchase cost of strategies 2 and 3 in multiple scenarios is relatively low, the cost of ESS allocation is higher, and the total cost is also higher, which verifies the effectiveness of the proposed hybrid ESS allocation strategy. In Fig. 11(c), strategy 3 only considers the normal operation of DNs, and ESSs are effectively allocated with less network loss, which verifies the correctness of the allocation strategy for the normal operation of the first step. In Fig. 11(d), The comparison of the total cost verifies the effectiveness of the proposed hybrid ESS allocation strategy. The results of Fig. 11 indicate that the ESSs in the proposed hybrid ESS allocation strategy has the highest utilization rate, and each ESS can achieve the maximum arbitrage with the TOU price.

In the four failure scenarios of Table IV, the movement of MESS between different load nodes can effectively ensure the uninterrupted power of critical loads in the DN. Figure 13 shows the comparison of the CLRR of the mobility mobile strategy with and without MESS in the DN in the four failure scenarios. It can be seen from Fig. 13 that although there are SESSs, the disconnection of the line will also cause the loss of power supply for critical loads. In the case of MESS allocation, while ensuring the uninterrupted power of critical loads in the region after the failure occurs, the movement of MESS ensures that all critical loads in the DN are uninterrupted, which can effectively improve the recovery rate of critical loads. MESS can guarantee a 100% recovery rate of critical loads within two hours of failure.

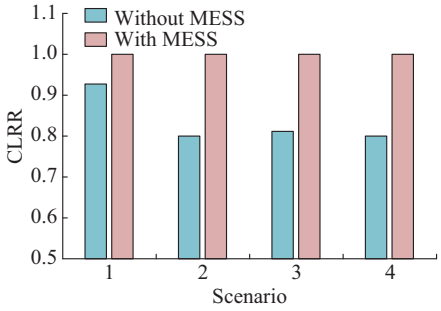

Fig. 13. Comparison of CLRR with and without MESS.

With the line failure shown in failure scenario 2 in Table IV, the failure recovery of the hybrid ESS allocation strategy is shown in Fig. 14 and the results of failure recovery are shown in Fig. 15. The ALLR of different allocation strategies mainly depends on the ESS allocation capacity. The allocation capacity of strategy 3 is larger, so the ALRR is higher. Due to the limitation of SESS capacity and the limitation of installed nodes, the CLLR of strategies 1-3 is relatively low.

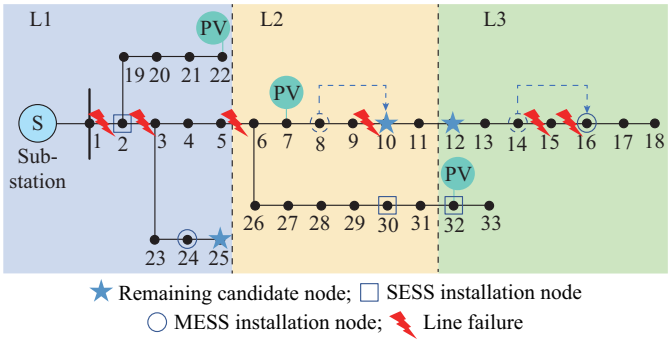

Fig. 14. Failure recovery of proposed hybrid ESS allocation strategy.

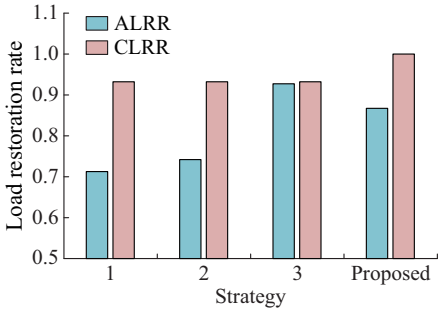

Fig. 15. Results of failure recovery.

As shown in Fig. 14, nodes 16-18 lose power supply; the MESS of node 8 in district 2 can be moved to node 10 to restore power; and node 16 in district 3 can be powered by moving MESS at node 14 to restore power supply. Therefore, the hybrid ESS allocation strategy guarantees the power supply reliability for important loads, which verifies the superiority of the proposed hybrid ESS allocation strategy.

V. Conclusion

To solve practical problems in ESS allocation, this paper proposes a two-step optimal allocation model of SESSs and MESSs. The allocations of the first step and the second step are optimized for the operation economy and the lowest cost of load loss considering the normal and failure operation conditions of DNs, respectively. A hybrid ESS allocation strategy based on subjective and objective weight analysis is proposed to give the final allocation results of SESSs and MESSs. The results of single SESS allocation and hybrid ESS allocation are compared and analyzed under the normal and failure operation conditions, which demonstrate that the proposed hybrid ESS allocation strategy can achieve lower annual operation cost in different scenarios as well as quick restorations of load power supply after failures. In summary, the proposed hybrid ESS allocation strategy would not only ensure the economic operation of the DN, but also maintain the power supply of the DN and improve the flexibility of the DN.

References

[1] H. T. Nguyen, J. W. Muhs, and M. Parvania, "Assessing impacts of energy storage on resilience of distribution systems against hurricanes," *Journal of Modern Power Systems and Clean Energy*, vol. 7, no. 4, pp. 731-740, Jul. 2019.

[2] Z. Lin, Z. Hu, H. Zhang *et al*., "Optimal ESS allocation in distribution network using accelerated generalized Benders decomposition," *IET Generation, Transmission & Distribution*, vol. 13, no. 13, pp. 2738-2746, Jan. 2019.

[3] Y. Zheng, Y. Song, A. Huang *et al*., "Hierarchical optimal allocation of battery energy storage systems for multiple services in distribution systems," *IEEE Transactions on Sustainable Energy*, vol. 11, no. 3, pp. 1911-1921, Jul. 2020.

[4] A. S. A. Awad, T. H. M. El-Fouly, and M. M. A. Salama, "Optimal ESS allocation for load management application," *IEEE Transactions on Power Systems*, vol. 30, no. 1, pp. 327-336, Jan. 2015.

[5] I. Naidji, M. B. Smida, M. Khalgui *et al*., "Efficient allocation strategy of energy storage systems in power grids considering contingencies," *IEEE Access*, vol. 7, pp. 186378-186392, Dec. 2019.

[6] N. Yan, B. Zhang, W. Li *et al*., "Hybrid energy storage capacity allocation method for active distribution network considering demand side response," *IEEE Transactions on Applied Superconductivity*, vol. 29, no. 2, pp. 1-4, Mar. 2019.

[7] A. S. A. Awad, T. H. M. El-Fouly, and M. M. A. Salama, "Optimal ESS allocation for benefit maximization in distribution networks," *IEEE Transactions on Smart Grid*, vol. 8, no. 4, pp. 1668-1678, Jul. 2017.

[8] A. Giannitrapani, S. Paoletti, A. Vicino *et al*., "Optimal allocation of energy storage systems for voltage control in LV distribution networks," *IEEE Transactions on Smart Grid*, vol. 8, no. 6, pp. 2859-2870, Nov. 2017.

[9] B. Li, X. Li, X. Bai *et al*., "Storage capacity allocation strategy for distribution network with distributed photovoltaic generators," *Journal of Modern Power Systems and Clean Energy*, vol. 6, no. 6, pp. 1234-1243, Nov. 2018.

[10] A. Jalali and M. Aldeen, "Risk-based stochastic allocation of ESS to ensure voltage stability margin for distribution systems," *IEEE Transactions on Power Systems*, vol. 34, no. 2, pp. 1264-1277, Mar. 2019.

[11] C. K. Das, O. Bass, T. S. Mahmoud *et al*., "An optimal allocation and sizing strategy of distributed energy storage systems to improve performance of distribution networks" *Journal of Energy Storage*, vol. 26, pp. 1-20, Dec. 2019.

[12] W. Ma, W. Wang, X. Wu *et al*., "Optimal allocation of hybrid energy storage systems for smoothing photovoltaic power fluctuations considering the active power curtailment of photovoltaic," *IEEE Access*, vol. 7, pp. 74787-74799, Jun. 2019.

[13] F. Mohammadi, H. Gholami, G. B. Gharehpetian *et al*., "Allocation of centralized energy storage system and its effect on daily grid energy generation cost," *IEEE Transactions on Power Systems*, vol. 32, no. 3, pp. 2406-2416, May 2017.

[14] J. Martinez-Rico, E. Zulueta, I. R. de Argandoña *et al*., "Multi-objective optimization of production scheduling using particle swarm optimization algorithm for hybrid renewable power plants with battery energy storage system," *Journal of Modern Power Systems and Clean Energy*, vol. 9, no. 2, pp. 285-294, Mar. 2021.

[15] S. Wen, H. Lan, Q. Fu *et al*., "Economic allocation for energy storage system considering wind power distribution," *IEEE Transactions on Power Systems*, vol. 30, no. 2, pp. 644-652, Mar. 2015.

[16] J. Chen, X. Jiang, J. Li *et al*., "Multi-stage dynamic optimal allocation for battery energy storage system in distribution networks with photovoltaic system," *International Transactions on Electrical Energy Systems*, vol. 30, no. 12, p. 12644, Dec. 2020.

[17] C. Thrampoulidis, S. Bose, and B. Hassibi, "Optimal placement of distributed energy storage in power networks," *IEEE Transactions on Automatic Control*, vol. 61, no. 2, pp. 416-429, Feb. 2016.

[18] M. Nick, R. Cherkaoui, and M. Paolone, "Optimal allocation of dispersed energy storage systems in active distribution networks for energy balance and grid support," *IEEE Transactions on Power Systems*, vol. 29, no. 5, pp. 2300-2310, Sept. 2014.

[19] R. Li, W. Wang, Z. Chen *et al*., "Optimal planning of energy storage system in active distribution system based on fuzzy multi-objective bi-level optimization," *Journal of Modern Power Systems and Clean Energy*, vol. 6, no. 2, pp. 342-355, Mar. 2018.

[20] B. Zhao, J. Ren, J. Chen *et al*., "Tri-level robust planning-operation co-optimization of distributed energy storage in distribution networks with high PV penetration," *Applied Energy*, vol. 279, p. 115768, Dec. 2020.

[21] H. Abdeltawab and Y. A. I. Mohamed, "Mobile energy storage sizing and allocation for multi-services in power distribution systems," *IEEE Access*, vol. 7, pp. 176613-176623, Dec. 2019.

[22] S. Yao, P. Wang, X. Liu *et al*., "Rolling optimization of mobile energy storage fleets for resilient service restoration," *IEEE Transactions on Smart Grid*, vol. 11, no. 2, pp. 1030-1043, Mar. 2020.

[23] J. Kim and Y. Dvorkin, "Enhancing distribution system resilience with mobile energy storage and microgrids," *IEEE Transactions on Smart Grid*, vol. 10, no. 5, pp. 4996-5006, Sept. 2019.

[24] H. H. Abdeltawab and Y. A. I. Mohamed, "Mobile energy storage scheduling and operation in active distribution systems," *IEEE Transactions on Industrial Electronics*, vol. 64, no. 9, pp. 6828-6840, Sept. 2017.

[25] Z. Lv, T. Liu, C. Shi *et al*., "Novel land cover change detection method based on *K*-means clustering and adaptive majority voting using bitemporal remote sensing images," *IEEE Access*, vol. 7, pp. 34425-34437, Jan. 2019.

[26] H. Gao, Y. Zhang, X. Ji *et al*., "Scenario clustering based distributionally robust comprehensive optimization of active distribution network," *Automation of Electric Power Systems*, vol. 44, no. 21, pp. 32-41, Nov. 2020.

[27] J. Chen, W. Zhang, J. Li *et al*., "Optimal sizing for grid-tied mi-

crogrids with consideration of joint optimization of planning and operation," *IEEE Transactions on Sustainable Energy*, vol. 9, no. 1, pp. 237-248, Jan. 2018.
[28] B. Zhao, H. Qiu, R. Qin *et al*., "Robust optimal dispatch of AC/DC hybrid microgrids considering generation and load uncertainties and energy storage loss," *IEEE Transactions on Power Systems*, vol. 33, no. 6, pp. 5945-5957, Nov. 2018.
[29] C. He, C. Dai, L. Wu *et al*., "Robust network hardening strategy for enhancing resilience of integrated electricity and natural gas distribution systems against natural disasters," *IEEE Transactions on Power Systems*, vol. 33, no. 5, pp. 5787-5798, Sept. 2018.
[30] Z. Lin, F. Wen, H. Wang *et al*., "CRITIC-based node importance evaluation in skeleton-network reconfiguration of power grids," *IEEE Transactions on Circuits and System II: Express Briefs*, vol. 65, no. 2, pp. 206-210, Feb. 2018.
[31] J. Wang, W. Pang, L. Wang *et al*., "Synthetic evaluation of steady-state power quality based on combination weighting and principal component projection method," *CSEE Journal of Power and Energy Systems*, vol. 3, no. 2, pp. 160-166, Jun. 2017.
[32] Y. Gao, X. Hu, W. Yang *et al*., "Multi-objective bilevel coordinated planning of distributed generation and distribution network frame based on multiscenario technique considering timing characteristics," *IEEE Transactions on Sustainable Energy*, vol. 8, no. 4, pp. 1415-1429, Oct. 2017.

Xinyi Jiang received the B.S. degree in electrical engineering from Yanshan University, Qinhuangdao, China, in 2019. She is currently working toward the M.S. degree with the Key Laboratory of Power System Intelligent Dispatch and Control of Ministry of Education, Shandong University, Jinan, China. Her research interests include distribution network resilience and optimal allocation of energy storage system.

Jian Chen received the B.S. degree from Shandong University, Jinan, China, in 2009, and the Ph.D. degree from Tianjin University, Tianjin, China, in 2014, both in electrical engineering. He has been working with Nanyang Technological University, Singapore, as a Research Fellow from Jan. 2015 to Jan. 2016. Now he is an Associate Professor with the Key Laboratory of Power System Intelligent Dispatch and Control of Ministry of Education, Shandong University. His research interests include energy storage system, integrated energy system, and cyber-physical system.

Qiuwei Wu received the Ph.D. degree in power system engineering from Nanyang Technological University, Singapore, in 2009. He was a Senior R&D Engineer with VESTAS Technology R&D Singapore Pte. Ltd., Singapore, from Mar. 2008 to Oct. 2009. He has been working at Department of Electrical Engineering, Technical University of Denmark (DTU), Lyngby, Denmark, since Nov. 2009 (Postdoctoral from Nov. 2009 to Oct. 2010, Assistant Professor from Nov. 2010 to Aug. 2013, and Associate Professor since Sept. 2013). He was a Visiting Scholar at Department of Industrial Engineering & Operations Research (IEOR), University of California, Berkeley, USA, from Feb. 2012 to May 2012, funded by the Danish Agency for Science, Technology and Innovation (DASTI), Copenhagen, Denmark. He was a Visiting Professor named by Y. Xue, an Academician of Chinese Academy of Engineering, at Shandong University, Jinan, China, from Nov. 2015 to Oct. 2017. He was a Visiting Scholar at the Harvard China Project, School of Engineering and Applied Sciences, Harvard University, Cambridge, USA, from Nov. 2017 to Oct. 2018 funded by the Otto Mønsted Fond. His research interests include operation and control of power systems with high penetration of renewables, including wind power modelling and control, active distribution networks, and operation of integrated energy systems.

Wen Zhang received the B.S., M.S., and Ph.D. degrees from Shandong University, Jinan, China, in 1989, 1992, and 2006, respectively, all in electrical engineering. She is currently a Professor with the Key Laboratory of Power System Intelligent Dispatch and Control of Ministry of Education, Shandong University. Her current research interests include power system analysis and control, demand-side response, and application of artificial intelligence in power systems.

Yicheng Zhang received the B.E. degree in automation from the Hefei University of Technology, Hefei, China, in 2011, the M.E. degree in pattern recognition and intelligent systems from the University of Science and Technology of China, Hefei, China, in 2014, and the Ph.D. degree in electrical and electronic engineering from Nanyang Technological University, Singapore, in 2019. Before joining Institute for Infocomm Research (I2R), Singapore, he was a Research Associate with Rolls-Royce@NTU Corporate Lab, Singapore. He is currently a Research Scientist with the I2R, Agency for Science, Technology and Research (A*STAR), Singapore. His current research interests include large-scale network optimization, intelligent transportation systems, and machine intelligence.

Jie Liu received the B.S. and M.S. degrees from Shandong University, Jinan, China, in 2009 and 2012, respectively, all in electrical engineering. He has been working in State Grid Yantai Power Supply Company, Yantai, China. His current research interests include power grid planning and energy optimization.